



# Structural and electrical properties of $\text{In}_{35}\text{Sb}_{45}\text{Se}_{20-x}\text{Te}_x$ chalcogenide thin films



A.K. Diab\*, M.M. Wakkad, E.Kh. Shokr, W.S. Mohamed

Physics Department, Faculty of Science, Sohag University, 82524 Sohag, Egypt

## ARTICLE INFO

### Article history:

Received 19 March 2014

Accepted 4 May 2015

### Keywords:

$\text{In}_{35}\text{Sb}_{45}\text{Se}_{20-x}\text{Te}_x$

Thin films

XRD

Electrical properties

Annealing temperature

## ABSTRACT

The structural and electrical properties of the as-prepared and annealed  $\text{In}_{45}\text{Sb}_{35}\text{Se}_{20-x}\text{Te}_x$  thin films with different compositions ( $x = 2.5, 5, 7.5, 10, 12.5$  and  $15$  at.%) prepared by electron beam evaporation method are studied. The XRD patterns of the as-prepared thin film show that the investigated compositions have amorphous and polycrystalline structure depending on the Te content. After annealing the  $\text{In}_{35}\text{Sb}_{45}\text{Se}_{20-x}\text{Te}_x$  thin films, at 473 K for 10 min, crystalline peaks are obtained. The electrical measurements were taken during heating in the range from 300 to 600 K. It was found that the resistivity decreases with increasing temperature for all the compositions indicating that these films have a semiconducting behavior. After annealing it was found that the room temperature resistivity of the investigated films were found depend on annealing temperature which cause a reduction by five orders of magnitude. These can be attributed to the amorphous–crystalline transformation, which is accompanied by a pronounced change in the electronic structure.

© 2015 Elsevier GmbH. All rights reserved.

## 1. Introduction

Glasses or films consisting of mixtures of elements such as Se, Te, Ge, Si, and Sb are electronic rather than ionic conductors, although their resistivities are usually high. The conductivity is thermally activated; that is, the conductivity increases exponentially with decreasing  $1/T$ , where  $T$  is the absolute temperature [1]. Hence, they are called semiconducting glasses. Chalcogenide films are new kind of materials with immense qualities of use in many practical applications. The chalcogenide materials are containing at least one of the chalogen elements, S, Se and/or Te. These materials exhibit unique infrared transmission and electrical properties, which makes them potentially useful for many applications such as threshold and memory switching [2]. Since a high-speed switching and the memory effect of an amorphous semiconductor were reported [3,4], its properties have been studied very actively. There have been many discussions on the mechanism of high speed switching and of electrical conduction in amorphous semiconductors. The study of the electrical properties is necessary to identify the electrical conduction mechanism occurring in the off state of chalcogenide glass switchers. One possible conduction mechanism is the space charge limited current [5], hopping

conduction [6], small polaron conduction [7] and the Poole–Frenkel conduction [8].

Indium antimonide (InSb) is the binary semiconductor in the III–V group having the lowest band gap. It has a band gap of 0.17 eV at 300 K corresponding to an infrared wavelength of 6.2  $\mu\text{m}$ . Another peculiarity of this material is its low effective electron mass and high mobility [9,10]. InSb has attracted several research groups because of the wide applications in magnetic sensors, infrared detectors as well as in infrared laser devices [11,12]. For device applications, amplification and signal processing are required. Usually it is done using discrete circuits, which are physically separated from the InSb sensor array [13].

Chalcogenide material systems such as In–Sb–Se, In–Sb–Te, Ge–Sb–Te, Ag–In–Sb–Te were studied [14–18]. Glass-formation, amorphization range and the information recording conditions for the amorphous layers of In–Sb–Se system (Sb–Se and  $\text{Sb}_2\text{Se}_3$ –InSb section) and the conditions of optical information recording on amorphous layers of  $(\text{Sb}_2\text{Se}_3)_x(\text{InSb})_{1-x}$  were studied [19]. But there is very little information on the addition of Te to In–Sb–Se ternary system. The system  $\text{In}_2\text{Se}_3$ – $\text{Sb}_2\text{Se}_3$  is a semiconducting compound with very interesting electrical properties, which has not been sufficiently investigated [20]. Few authors studied electrical properties of  $\text{InSbSe}_3$  single crystal [21,22]. Every material has a unique set of electrical characteristics that are dependent on its dielectric properties. Accurate measurements of the electrical properties can provide scientists and engineers with valuable

\* Corresponding author. Tel.: +20 934601159; fax: +20 9304601159.

E-mail address: [diab.a.k@yahoo.com](mailto:diab.a.k@yahoo.com) (A.K. Diab).

information to properly incorporate the material into its intended applications for more solid design or to monitor a manufacturing process for improved quality control. Therefore, in this study we examine the electrical properties of the as-prepared and annealed  $\text{In}_{45}\text{Sb}_{35}\text{Se}_{20-x}\text{Te}_x$  thin films.

## 2. Experimental procedures

Bulk samples of  $\text{In}_{35}\text{Sb}_{45}\text{Se}_{20-x}\text{Te}_x$  ( $x = 2.5, 5, 7.5, 10, 12.5$  and  $15 \text{ at.\%}$ ) were prepared using a conventional melt quenching technique [23]. Typical, 10 g total (per batch) of appropriate quantities of 99.999% pure indium (In), antimony (Sb), selenium (Se) and tellurium (Te) were weighted according to their atomic percentages and sealed in quartz ampoules in a vacuum of  $\approx 10^{-5}$  Torr. The sealed ampoules were kept inside a furnace where the temperature was increased up to 1000 K for about 24 h. During the preparation the ampoules were continuously rotated to ensure complete mixing of the various constituents. At the end the ampoules were quenched in the ice water to obtain the glasses.

Thin films of the considered compositions were prepared by electron beam evaporation, in an Edward's high vacuum coating unit model 306 A at a pressure of  $5 \times 10^{-6}$  and  $8 \times 10^{-5}$  Torr before and during film deposition, respectively. The films were prepared on ultrasonically cleaned microscopic glasses held at room temperature. The thickness ( $d$ ) of the films ( $\approx 25\text{--}150 \text{ nm}$ ) was controlled using digital film thickness monitor model TM 200 Maxtek. The deposition rate was  $\approx 7 \text{ nm/s}$ . The crystallographic structure of the as-prepared films was determined by X-ray diffraction (XRD) using a Philips X'pert MRD diffractometer.  $\text{CuK}_\alpha$  radiation ( $\lambda = 1.541837 \text{ \AA}$ ) was used from the X-ray tube with grazing incidence. The angle of incidence was  $0.75^\circ$ .

Atomic force microscopy (AFM) of the as-prepared films was determined by the scanned probe microscopy (SPM) family of instruments. In these SPM techniques a small probe (10–100 nm radius of curvature) is raster scanned by a piezoelectric device over a sample to produce an image of the sample surface, or near surface region.

The direct conductivity, d.c., ( $\sigma$ ) were determined from the measurements of film resistance. The film resistance measurement was carried out using a two-terminal configuration; the measurements were carried out in a well-controlled quartz tube furnace combined with a digital Keithley 614 electrometer. The measurements were achieved under argon flow in the temperature range 303–573 K. Electrical contacts were made by applying silver paste over the surface of the thin films (as-deposited and/or annealed) with separation of about 2.5 mm. To avoid silver diffusion in to the gap we used different similar films and applied the silver paste after annealing.

## 3. Results and discussion

### 3.1. XRD characterization

The XRD patterns of the as-prepared thin film (thickness 150 nm) as a representative example were investigated [23]. It was found that the as-prepared compositions have amorphous or polycrystalline natures, which depend on Te content in the composition. The obtained pattern indicated that,  $\text{In}_{45}\text{Sb}_{35}\text{Se}_{17.5}\text{Te}_{2.5}$ ,  $\text{In}_{45}\text{Sb}_{35}\text{Se}_{15}\text{Te}_5$  and  $\text{In}_{45}\text{Sb}_{35}\text{Se}_{12.5}\text{Te}_{7.5}$  thin films are amorphous, while in each  $\text{In}_{45}\text{Sb}_{35}\text{Se}_{10}\text{Te}_{10}$ ,  $\text{In}_{45}\text{Sb}_{35}\text{Se}_{7.5}\text{Te}_{12.5}$  and,  $\text{In}_{45}\text{Sb}_{35}\text{Se}_5\text{Te}_{15}$  patterns crystalline peaks are obtained. From the JCPDS files, these peaks can be identified as  $\text{Sb}_2\text{Se}_3$  (card Nos. 22-0067 and 72-1184) and  $\text{Sb}_2\text{SeTe}_2$  (card No.38-0979) crystalline phases [23].

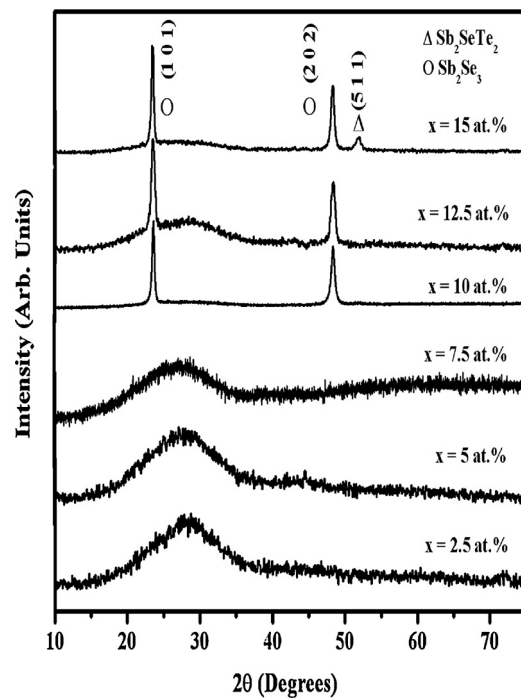


**Fig. 1.** XRD patterns of  $\text{In}_{35}\text{Sb}_{45}\text{Se}_{20-x}\text{Te}_x$  thin films annealing at 473 K for 10 min.

After annealing the  $\text{In}_{35}\text{Sb}_{45}\text{Se}_{20-x}\text{Te}_x$  thin films at 473 K for 10 min, crystalline peaks are obtained (Fig. 1). From the JCPDS files these peaks can be identified as  $\text{Sb}_2\text{Se}_3$  (card No. 15-0861 and 72-1184), and  $\text{Sb}_2\text{SeTe}_2$  (card No. 39-0776) crystalline phases. With increasing Te content the intensity of these peaks decrease, and a new peaks were appeared. From the JCPDS files these peaks can be identified as  $\text{InSb}$  (card No. 22-0067), and  $\text{Sb}_2\text{SeTe}_2$  (card Nos. 38-0979 and 27-0025) crystalline phases and the intensity of these peaks increases with increasing Te content. The mentioned behavior can be attributed to the increases of Te in the compositions.

### 3.2. Surface studies

The surface topography and roughness has been investigated using AFM. The root mean square (RMS) roughness was calculated for the films with different Te content. Fig. 2 shows the

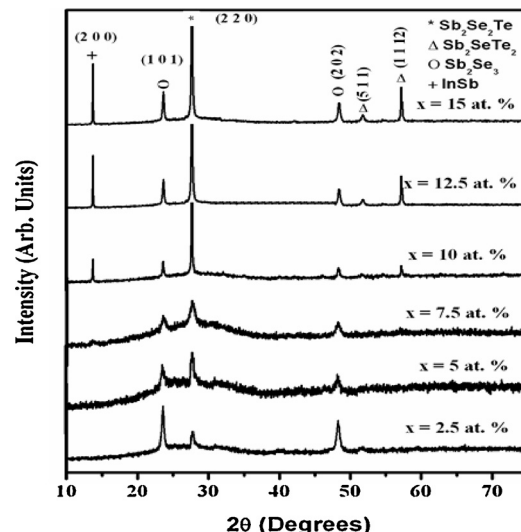


**Fig. 2.** AFM image of as-prepared  $\text{In}_{45}\text{Sb}_{35}\text{Se}_{17.5}\text{Te}_{2.5}$  thin films.

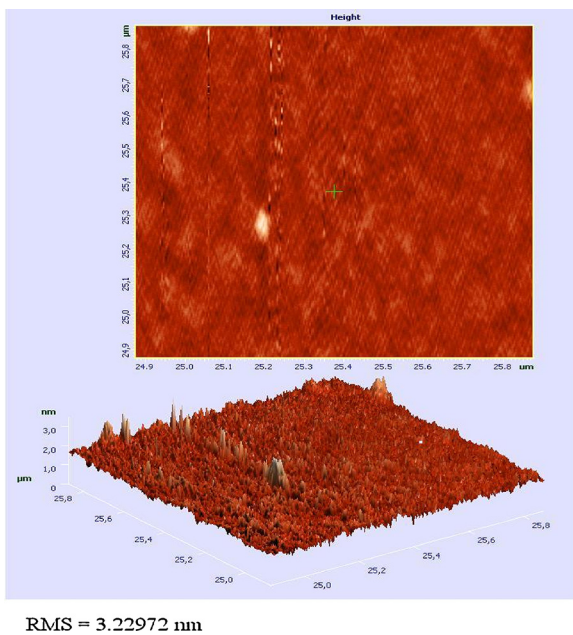


**Fig. 3.** AFM image of as-prepared  $\text{In}_{45}\text{Sb}_{35}\text{Se}_{15}\text{Te}_{5}$  thin films.

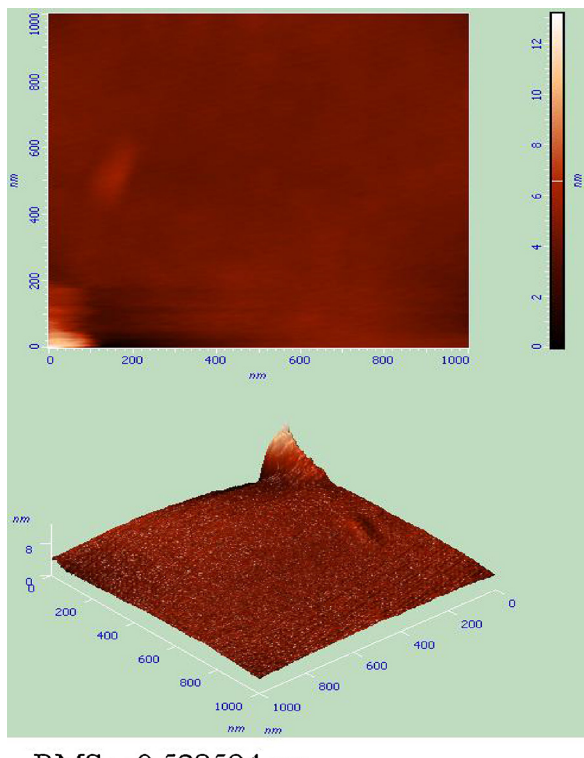


**Fig. 5.** AFM image of as-prepared  $\text{In}_{35}\text{Sb}_{45}\text{Se}_{7.5}\text{Te}_{12.5}$  thin films.

surface morphology of as-prepared  $\text{In}_{35}\text{Sb}_{45}\text{Se}_{17.5}\text{Te}_{2.5}$  thin film. It was found that the RMS roughness of this film is the highest one which has RMS roughness of 3.2 nm and the surface of the film grew in the form of needles. Such behavior was reported for other phase change materials such as Bi–Ge–Sb–Te films [24]. Figs. 3–5 show the surface morphology of as-prepared  $\text{In}_{35}\text{Sb}_{45}\text{Se}_{15}\text{Te}_5$ ,  $\text{In}_{35}\text{Sb}_{45}\text{Se}_{12.5}\text{Te}_{7.5}$  and  $\text{In}_{35}\text{Sb}_{45}\text{Se}_{7.5}\text{Te}_{12.5}$  thin films, respectively. It found that the surface roughness was 1.2, 0.52 and 0.2 nm, respectively. The main conclusion of AFM investigation is that the roughness was decreased with increasing Te content, i.e. with decreasing of Se content which in turn the decrease of Se atoms towards the surface [25].

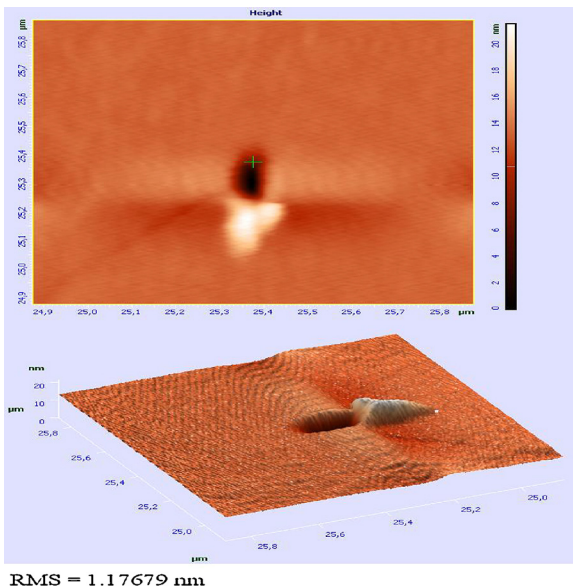


**Fig. 4.** AFM image of as-prepared  $\text{In}_{45}\text{Sb}_{35}\text{Se}_{12.5}\text{Te}_{7.5}$  thin films.

### 3.3. Electrical properties of the as-prepared thin films

The effect of Te content on the electrical conductivity of the as-prepared  $\text{In}_{35}\text{Sb}_{45}\text{Se}_{20-x}\text{Te}_x$  ( $x = 2.5, 5, 7.5, 10, 12.5$  and 15 at.%) thin films of thickness 150 nm deposited on glass substrate held at room temperature were studied. Measurements were taken during heating from room temperature (300 K) up to 600 K. The values of the room temperature resistance,  $\rho_{rm}$ , are shown in Fig. 6. It was found that the resistance of the  $\text{In}_{35}\text{Sb}_{45}\text{Se}_{17.5}\text{Te}_{2.5}$  composition is very high ( $7.54 \times 10^5 \Omega$ ) and decrease quickly with increasing Te content. Fig. 7 shows the variations of resistivity with temperature. It was found that the resistivity decreases with increasing temperature for all the compositions indicating that these films have a semiconducting behavior. From Fig. 7 it is clear that the resistivity at low temperature is high. These can be attributed to that the most of the carriers are frozen out on the acceptor and donor levels. As the temperature rises, the degree of ionization of the impurities increases, and the raise of the carrier concentration results in a rapidly decrease of the resistivity. At higher temperature, the resistivity shows a flat minimum at about 450 K, followed at still higher temperature by a tendency to decrease. The reason for the tendency lies in the temperature dependence of the mobility. In this temperature range, the films exhibit a metallic behavior. Hence, the mobility of the carriers decreases with raising the temperature because of the lattice scattering. The increase of the thermal agitation of the lattice causes shorter distances of the carriers between collisions, and the carriers travel faster, thus reducing the time between collisions. Both these facts cause the decrease of the mobility. The step change around 450 K can be related to the amorphous–crystalline transformation which is accompanied by a pronounced change in electronic structure [26]. This amorphous–crystalline transformation confirmed by XRD examinations where crystalline peaks could be observed above 450 K.

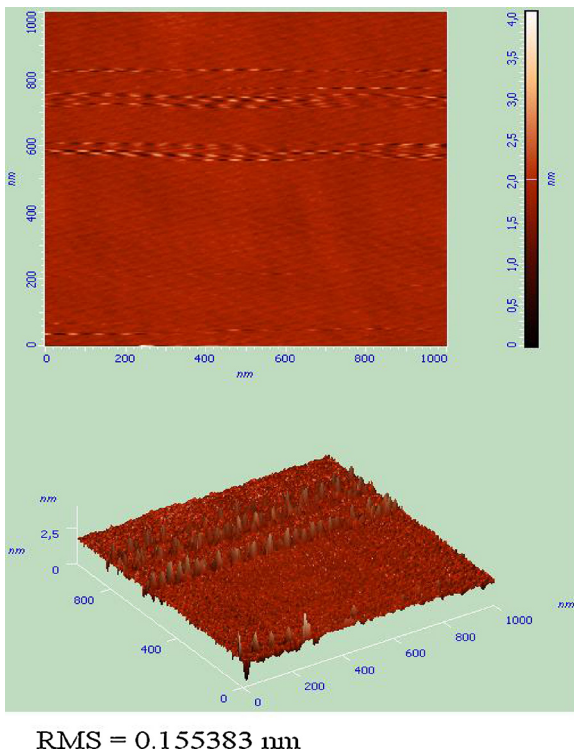


**Fig. 6.** Variations of room temperature resistivity in ( $\Omega$  cm) of  $\text{In}_{35}\text{Sb}_{45}\text{Se}_{20-x}\text{Te}_x$  thin films with Te content.

The electrical conductivity  $\sigma$  can be written as an exponential function of temperature ( $T$ ),

$$\sigma(T) = \sigma_0 \exp(-E_A/k_B T) \quad (1)$$

where  $E_A$  is the activation energy for electrical conduction, which is a function of the electronic energy levels of the chemically interacting atoms in the amorphous materials and hence of the emerging band gap,  $\sigma_0$  is the pre-exponential factor including the charge of carrier mobility and density of states, and  $k_B$  is the Boltzmann constant. The activation energy can be derived from the logarithmic plot of such dependence (Fig. 8). The linear fit was taken only for the linear portion. The value of  $E_A$  and  $\sigma_0$  for  $\text{In}_{35}\text{Sb}_{45}\text{Se}_{20-x}\text{Te}_x$  films with various Te content are compiled in Table 1. It was found that, both the activation energy and pre-exponential factor increased with further substitution of Se with Te in the sample. The observed increase in activation energy for sample with higher tellurium content might be related to statistical shift of Fermi level with the

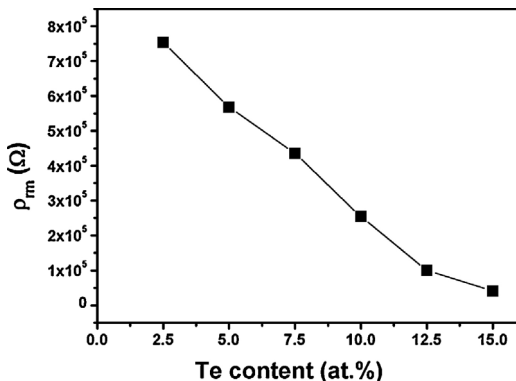


**Fig. 7.** Variation of resistivity in  $\Omega$  cm of  $\text{In}_{35}\text{Sb}_{45}\text{Se}_{20-x}\text{Te}_x$  thin films with the ambient temperature.

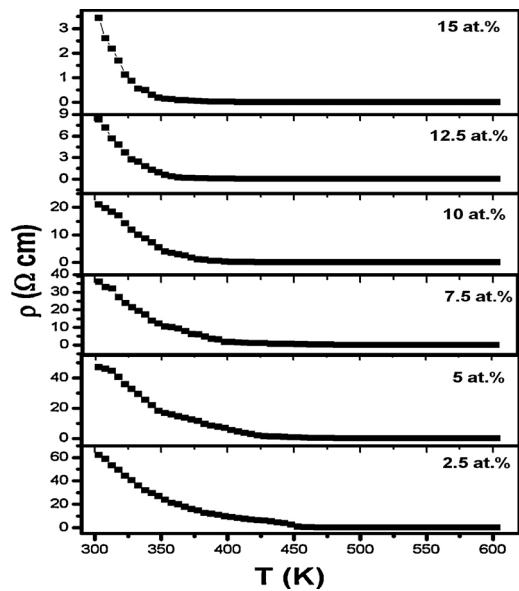


**Fig. 8.** Arrhenius plot of the conductivity,  $\ln(\sigma)$  versus  $1000/T$ ,  $\sigma$  in  $\Omega^{-1} \text{ cm}^{-1}$ , for  $\text{In}_{35}\text{Sb}_{45}\text{Se}_{20-x}\text{Te}_x$  films prepared at various Te content.

increase of tellurium content in the material, and might be related to amorphous to crystalline transformation in these compositions.

The observed higher values of pre-exponential factor  $\sigma_0 > 88 \Omega^{-1} \text{ cm}^{-1}$  for as-prepared thin films represents the conduction of charge carriers through extended states constituting the valence and conduction bands [27]. The pre-exponential values also showed a sharp decrease of two orders of magnitude for initial substitution of Se with Te. Further tellurium substitution showed insignificant changes in the pre-exponential factor.

#### 3.4. Effect of annealing on the electrical properties

To study the effect of annealing temperature (for 10 min) on the electrical conductivity of for  $\text{In}_{35}\text{Sb}_{45}\text{Se}_{20-x}\text{Te}_x$  films, at first we consider the dependence of room temperature resistivity on  $T_{\text{an}}$ . Fig. 9 shows the dependence of room temperature resistivity of  $\text{In}_{35}\text{Sb}_{45}\text{Se}_{20-x}\text{Te}_x$  system on  $T_{\text{an}}$ . In general,  $\rho_{rm}$  decreases with increasing the annealing temperature but the decrease is steeper when annealing at 473 K. Further annealing, above 473 K, results in a gradual decrease of the  $\rho_{rm}$ . The total reduction in  $\rho_{rm}$  is of five orders of magnitude. This large decrease in  $\rho_{rm}$  upon annealing was previously reported for other chalcogenide thin film such as  $\text{Sb}_x\text{Se}_{100-x}$  ( $60 \leq x \leq 70$ ) [28],  $\text{Ge}_4\text{Sb}_1\text{Te}_5$  [26] and  $\text{Se}_{75}\text{Te}_{15}\text{Sn}_{10}$  [29] and it can be related to the amorphous-crystalline transformation which is accompanied by a pronounced change in electronic structure [26]. Such transformation is emphasized from XRD diffraction. The values of  $E_A$  calculated from plots of  $\ln(\sigma)$  versus  $1000/T$  as an example for same compositions of  $\text{In}_{35}\text{Sb}_{45}\text{Se}_{20-x}\text{Te}_x$  thin films annealed at different temperature are shown in Fig. 10. The  $E_A$  values decreases with increasing annealing temperature. This result

**Table 1**

Electrical activation energy ( $E_A$ ) and the pre-exponential factor ( $\sigma_0$ ) for the  $\text{In}_{35}\text{Sb}_{45}\text{Se}_{20-x}\text{Te}_x$  thin film.

X at.%	$E_A$ (eV)	$\sigma_0$ ( $\Omega^{-1} \text{ cm}^{-1}$ )
2.5	0.230	88.373
5	0.329	$3.5 \times 10^3$
7.5	0.406	$4.7 \times 10^4$
10	0.660	$1.09 \times 10^9$
12.5	0.728	$5.28 \times 10^{10}$
15	0.630	$5.8 \times 10^9$

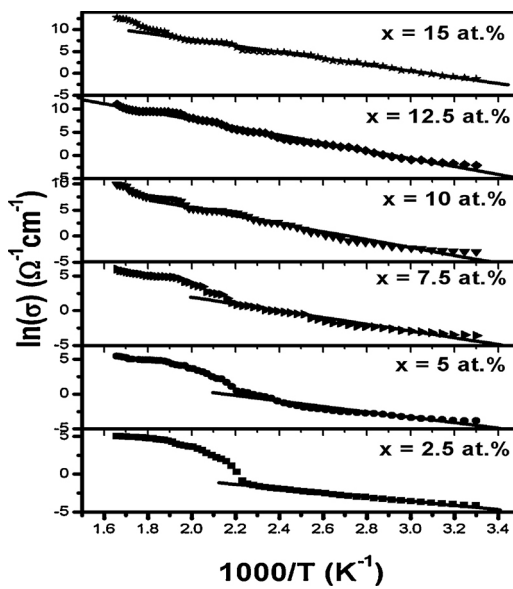


**Fig. 9.** Room temperature resistivity of  $\text{In}_{35}\text{Sb}_{45}\text{Se}_{20-x}\text{Te}_x$  system versus  $T_{\text{an}}$ . The solid line is a guide for the eye only.

can be ascribed to the phase transformation (amorphous to crystalline). Another reason which could account for the decrease in activation energy upon annealing is the decrease in forbidden band gap. The same behavior was reported for other chalcogenide thin film such as  $\text{CuSbTe}_2$  and  $\text{CuSbSe}_2$  [30] and  $\text{Sn}_x\text{Sb}_{20}\text{Se}_{80-x}$  ( $8 \leq x \leq 18$ ) [31].

Many researchers have reported different trends for variation of forbidden band gap and activation energy with annealing and different explanations have been given for the observed variation [32,33]. The difference in the observed trends might be due to different growth/annealing conditions for different systems. Some researchers have reported opposite variation of forbidden band gap and dc-activation energy with annealing [34]. In the present case the observed decrease in both forbidden band gap and dc-activation energy with annealing represents structural changes happening

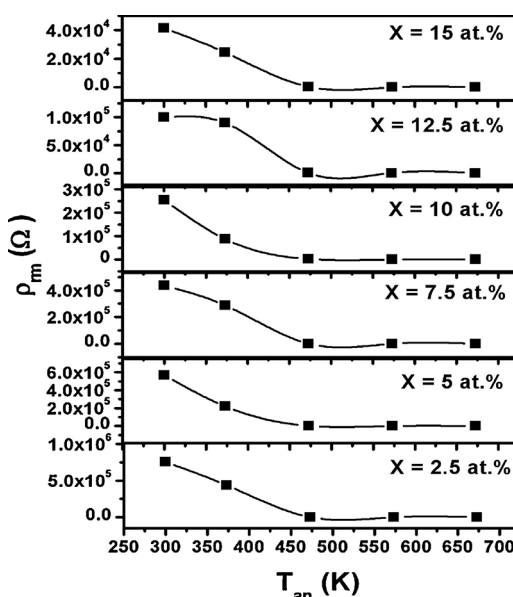


**Fig. 10.** Variation of the activation energy for electrical conduction of  $\text{In}_{35}\text{Sb}_{45}\text{Se}_{20-x}\text{Te}_x$  system as a function of  $T_{\text{an}}$ . The solid line is a guide for the eye only.

**Table 2**

Pre-exponential factor ( $\sigma_0$ ), calculated from plots of  $\ln(\sigma)$  versus  $1000/T$  for  $\text{In}_{35}\text{Sb}_{45}\text{Se}_{20-x}\text{Te}_x$  thin films annealed at different temperatures.

$T_{\text{an}}$ (K)	$\sigma_0 (\Omega^{-1} \text{cm}^{-1})$		
	X = 2.5 at.%	X = 7.5 at.%	X = 12.5 at.%
300	88.373	$4.7 \times 10^4$	$5.82 \times 10^9$
373	87.733	$28.91 \times 10^1$	$51.8 \times 10^3$
473	$16.45 \times 10^2$	$74.9 \times 10^1$	$27.98 \times 10^4$
573	$14.2 \times 10^3$	$3.848 \times 10^3$	$8.68 \times 10^3$

in the material associated with annealing process. According to Mott and Davis [27], the density of localized states within mobility gap is directly related to disorder due to unsaturated dangling bonds present in the system and observed decrease in optical band gap and dc-activation energy due to annealing might be related to increase in density of unsaturated dangling bonds which can be corroborated with the two order of magnitude decrease in pre-exponential factor  $\sigma_0$  associated with conduction for annealed films indicating the contribution of conduction of charge carriers through localized states.

The values of  $\sigma_0$  calculated from plots of  $\ln(\sigma)$  versus  $1000/T$  for  $\text{In}_{35}\text{Sb}_{45}\text{Se}_{20-x}\text{Te}_x$  thin films annealed at different temperature are listed in Table 2. It is seen that  $\sigma_0$  values show non-sequential dependence on  $T_{\text{an}}$ . However this observation can be attributed to the unsequential change in the microstructure of the investigated compositions.

#### 4. Conclusions

The structural and electrical properties of the  $\text{In}_{35}\text{Sb}_{45}\text{Se}_{20-x}\text{Te}_x$  thin films prepared by electron beam evaporation were investigated. The XRD characteristics showed that the as-prepared  $\text{In}_{35}\text{Sb}_{45}\text{Se}_{20-x}\text{Te}_x$  compositions have an amorphous and polycrystalline future depended on Te content in the composition. After annealing the  $\text{In}_{35}\text{Sb}_{45}\text{Se}_{20-x}\text{Te}_x$  thin films at 473 K for 10 min, crystalline peaks are obtained. It was found that the resistivity decreases with increasing temperature for all the compositions indicating that these films have a semiconducting behavior. The room temperature resistivity of  $\text{In}_{35}\text{Sb}_{45}\text{Se}_{20-x}\text{Te}_x$  system decreases with increasing the annealing temperature, these finding can be related to the amorphous-crystalline transformation which is accompanied by a pronounced change in electronic structure.

#### References

- [1] B.T. Kolomiets, Phys. Status Solidi 7 (1964) 713.
- [2] A.N. Sreeram, A.K. Varshneya, D.R. Swiler, J. Non Cryst. Solids 130 (1991) 225.
- [3] S.R. Ovshinsky, Phys. Rev. Lett. 21 (1968) 1450.
- [4] F.M. Collins, J. Non Cryst. Solids 2 (1970) 496.
- [5] J.L. Hartke, Phys. Rev. 125 (1962) 1177.
- [6] B.J. Bagley, Solid State Commun. 2 (1972) 4663.
- [7] D. Emin, C.H. Seager, P.K. Quinn, Phys. Rev. Lett. 28 (1972) 813.
- [8] R.M. Hill, Philos. Mag. 23 (1972) 59.
- [9] B.V. Rao, D. Gruenav, T. Tambo, C. Tatsuyama, Semicond. Sci. Technol. 16 (2001) 216.
- [10] R.A. Stradling, Braz. J. Phys. 26 (1996) 7.
- [11] G. Finger, R.J. Dorn, M. Meyer, L. Mehrgen, J. Stegmeier, A. Moorwood, Nucl. Instrum. Methods A549 (2005) 79.
- [12] A. Okamoto, T. Yoshida, S. Muramatsu, I. Shibusaki, J. Cryst. Growth 201 (1999) 765.
- [13] R. Sreekumar, P.M. Ratheesh Kumar, C. Sudha Kartha, K.P. Vijayakumar, D. Kabilraj, S.A. Khan, D.K. Avasthi, Y. Kashiwaba, T. Abe Semicond. Sci. Technol. 21 (2006) 382.
- [14] T. Ohta, J. Optoelectron. Adv. Mater. 3 (2001) 609.
- [15] A.M. Ahmed, N.M. Megahid, M.M. Wakkad, A.K. Diab, J. Phys. Chem. Solids 66 (2005) 1274.
- [16] N.K. Rana, J.N. Prasad, Indian J. Phys. 86 (2012) 601.
- [17] R.R. Pawar, R.A. Bhavsar, S.G. Sonawane, Indian J. Phys. 86 (2012) 871.
- [18] A.M. Ahmed, M.M. Wakkad, S.H. Mohamed, A.K. Diab, Indian J. Phys. 87 (2013) 317.

- [19] V.M. Rubish, P.P. Shtets, V.V. Rubish, D.G. Semak, B.R. Tsizh, J. Optoelectron. Adv. Mater. 5 (2003) 1193.
- [20] Belotskii F.D.P., P.F. Babyuk, N.V. Demyanchuk, Low Temperature Termoelectric Materials, Kishinev, 1970, pp. 29 (in Russian).
- [21] M. Spiesser, R.P. Gruska, S.N. Subbarao, C.A. Castro, A. Wold, J. Solid State Chem. 26 (1978) 111.
- [22] I. Kuliyeva, L.Kh. Khasanova, N.M. Salimova, Izv. Akad. Nauk Azerh SSR Ser. Fiz. Tekh. Mat. Nauk (USSR) 5 (1986) 87.
- [23] A.K. Diab, M.M. Wakkad, E.Kh. Shokr, W.S. Mohamed, J. Phys. Chem. Solids 71 (2010) 1381.
- [24] S.-S. Lin, Mater. Sci. Eng. B 129 (2006) 116.
- [25] T. Çolakoğlu, M. Parlak, Appl. Surf. Sci. 254 (2008) 1569.
- [26] D. Wamwangi, W.K. Njoroge, M. Wuttig, Thin Solid Films 408 (2002) 310.
- [27] N.F. Mott, E. Davis, Electronic Properties of Non-Crystalline Materials, Clarendon, Oxford, 1979.
- [28] M.J. Kang, S.Y. Choi, D. Wamwangi, K. Wang, C. Steimer, M. Wuttig, J. Appl. Phys. 98 (2005) 014904.
- [29] P. Sharma, S.C. Katyal, Mater. Lett. 61 (2007) 4516.
- [30] I.L. Soliman, M.A. Abo El Soad, H.A. Zayed, S.A. El Ghfar, Fizika A11 4 (2002) 139.
- [31] M.M. Wakkad, E.Kh. Shokr, H.A. Abd El Ghani, M.A. Awad, Eur. Phys. J. Appl. Phys. 43 (2008) 23.
- [32] Y. Kuzukawa, A. Ganjoo, K. Shimakawa, J. Non Cryst. Solids 227 (1998) 715.
- [33] A.A. Abu-sehly, M.I. Abd-Elrahman, J. Phys. Chem. Solids 63 (2002) 163.
- [34] A.S. Soltan, Appl. Phys. A 80 (2005) 117.